MATCH
Communications in Mathematical and in Computer Chemistry

MATCH Commun. Math. Comput. Chem. **90** (2023) 609–648
ISSN: 0340–6253
doi: 10.46793/match.90-3.609X

Extended Hybrid Controller Design of Bifurcation in a Delayed Chemostat Model

Changjin Xu[a], Qingyi Cui[b], Zixin Liu[b*], Yuanlu Pan[c], Xiaohan Cui[c], Wei Ou[b], Mati ur Rahman[d], Muhammad Farman[e], Shabir Ahmad[f], Anwar Zeb[g]

[a] *Guizhou Key Laboratory of Economics System Simulation, Guizhou University of Finance and Economics, Guiyang 550025, PR China*

[b] *School of Mathematics and Statistics, Guizhou University of Finance and Economics, Guiyang 550025, PR China*

[c] *Library, Guizhou University of Finance and Economics, Guiyang 550025, PR China*

[d] *School of Mathematical Science, Shanghai Jiao Tong University, Shanghai 200240, PR China*

[e] *Department of Mathematics, Khawaja Fareed University of Engineering and Information Technology, Rahim Yar Khan, Pakistan*

[f] *Department of Mathematics, University of Malakand, Chakdara, Dir Lower, Khyber Pakhtunkhwa, Pakistan*

[g] *Department of Mathematics, COMSATS University Islamabad, Abbottabad Campus, Abbottabad, 22060, Khyber, Pakhtunkhwa, Pakistan*

xcj403@126.com, cqy5388427@163.com, xinxin905@126.com, 137415148@qq.com, cuixiaohan2011@126.com, ouyiyich@163.com, mati-maths_374@sjtu.edu.cn, farmanlink@gmail.com, shabirahmad2232@gmail.com, anwar@cuiatd.edu.pk

(Received May 13, 2023)

*Corresponding author.

Abstract

Fractional-order differential models plays a pivotal role in depicting the relationship among concentration changes of various chemical substances in chemistry. In this current study, we will explore the dynamics of a delayed chemostat model. First of all, we prove that the solution of the delayed chemostat model exists and is unique by virtue of fixed point theorem. Secondly, we demonstrate that the solution of the delayed chemostat model is non-negative by applying some suitable inequality strategies. Thirdly, the boundedness of the solution to the delayed chemostat model is explored via constructing a reasonable function. Fourthly, the Hopf bifurcation and stability of the delayed chemostat model are dealt with by exploiting the stability criterion and bifurcation theory on fractional dynamical system. Fifthly, the stability domain and Hopf bifurcation of the delayed chemostat model are resoundingly controlled by making use of an extended hybrid controller. Sixthly, the stability domain and Hopf bifurcation of the delayed chemostat model are effectively adjusted by making use of an another extended hybrid controller. The role of delay in this chemostat model is revealed. Seventhly, software experiments are given to illustrate the rightness of the gained key conclusions. The acquired outcomes of this work are perfectly innovative and have crucial theoretical value in controlling the concentrations of various chemical substances.

1 Introduction

During the past several decades, a lot of researchers have established various mathematical models to explore the the inherent law in biological systems and chemical reactions. In particular, differential dynamical model plays a vital role in describing the interaction of the concentrations of different chemical substances. Up to now, a great deal of works on chemical reaction models have been proposed and investigated. Rich achievements on the dynamics of many chemical reaction models have been achieved. For example, Eskandari et al. [1] investigated the Neimark-Sacker bifurcation of a discrete chemical system and obtained the parameter condition to ensure the onset of Neimark-Sacker bifurcation; Zhang and He [2] dealt with the delay-induced Hopf bifurcation for a Lengyel-Epstein chemical reaction model and set up the sufficient condition ensuring the stability and onset of Hopf bifurcation of the model; Xu and Wu [3] carried out detailed analysis on Hopf bifurcation and chaos control issue for a chemical model; Lengyel et al. [4] studied the chemical oscillations of the chlorine dioxide-iodine-malonic acid reaction; In 2018, Din et al. [5] analyzed the stability, Neimark-Sacker bifurcation and chaos control issue for chlorine dioxide-iodine-malonic acid reaction model; Xu et al. [6] discussed the Hopf bifurcation and its control theory for a fractional-order Brusselator chemical reaction model owing time delay. In details, one can see [7–12].

In chemistry, chemostat model plays a vital role in understanding the growth law of cell mass in chemostat [13]. A chemostat can be regards as a reactor owing continuous inflow and outflow and stirred and providing effective mixing [12, 13]. The chemostat has a very important effect on interaction mechanism of various organisms in biological systems. Thus the exploration on chemostat models has attracted great interest from numerous scholars. In 2005, Nelson and Sidhu [13] proposed the following chemostat model:

$$\begin{cases} \dfrac{dw_1(t)}{dt} = qw_{10} - qw_1(t) - \dfrac{\mathcal{N}(w_1(t))w_2(t)}{\mathcal{Y}(w_1(t))}, \\ \dfrac{dw_2(t)}{dt} = qw_{20} - qw_2(t) + \mathcal{N}(w_1(t))w_2(t), \end{cases} \tag{1}$$

where w_1, w_2 represent substrate concentration, cell mass concentration, respectively; w_{10}, w_{20} represent initial substrate concentration, initial cell mass concentration, respectively; q stands for dilution rate; q, w_{10}, w_{20} are positive constants; $\mathcal{Y}$ denotes yield parameter; $\mathcal{N}(w_1(t))$(i.e., Monod growth model) denotes specific growth rate, which usually relies on the substrate concentration and takes the following form:

$$\mathcal{N}(w_1(t)) = \frac{uw_1(t)}{\kappa + w_1(t)}, \tag{2}$$

where κ denotes Monod constant and u denotes the maximum specific growth rate; κ, u are positive constants. The yield parameter $\mathcal{Y}$ takes the form:

$$\mathcal{Y}(w_1(t)) = r + bw_1(t), \tag{3}$$

where r, b are real positive constants. In many cases, time delay often occurs in the chemical reaction process. The the variation of temperature has an important effect on the growth of cell mass. Motivated by this viewpoint and assuming that the initial concentration of the cell mass $w_{20} = 0$, Mohd Aris and Jamaian [14] proposed the following delayed chemostat model:

$$\begin{cases} \dfrac{dw_1(t)}{dt} = qw_{10} - qw_1(t) - \dfrac{uw_1(t)w_2(t)}{(\kappa + w_1(t))(r + bw_1(t))}, \\ \dfrac{dw_2(t)}{dt} = -qw_2(t) + \dfrac{uw_1(t-\vartheta)w_2(t-\vartheta)}{\kappa + w_1(t-\vartheta)}, \end{cases} \tag{4}$$

where ϑ denotes a delay. In order to further describe the memory function and hereditary advantage of the concentrations of different chemical reactants, Mohd Aris and Jamaian [14] further set up the following fractional-order delayed chemostat model:

$$\begin{cases} \dfrac{d^\eta w_1(t)}{dt^\eta} = qw_{10} - qw_1(t) - \dfrac{uw_1(t)w_2(t)}{(\kappa + w_1(t))(r + bw_1(t))}, \\ \dfrac{d^\eta w_2(t)}{dt^\eta} = -qw_2(t) + \dfrac{uw_1(t-\vartheta)w_2(t-\vartheta)}{\kappa + w_1(t-\vartheta)}, \end{cases} \tag{5}$$

where $\eta \in (0, 1]$ denotes the fractional-order. Relying on the fractional-order dynamical theory, Mohd Aris and Jamaian [14] explored the stability issue numerically. Tt is a pity that the work of Mohd Aris and Jamaian [14] are not concerned with the dynamical behavior of the integer-order case, that is to say, Mohd Aris and Jamaian [14] did not investigated the dynamical behavior for model (4). In order to make up for this defect, we will deal with the dynamical behavior of system (4).

For various dynamical behaviors of delayed systems, delay-driven Hopf bifurcation plays a significant role in delayed dynamical models [15–20]. In chemistry, delay-driven Hopf bifurcation is able to effectively describe the balanced relations of the concentration of various chemical substances. Thus it is very important to investigate the delay-driven Hopf bifurcation in all sort of chemical reaction models. Stimulated by this viewpoint above, we will deal with the delay-driven Hopf bifurcation and its control aspect of model (4). In particular, we will focus on the following key topics: **(i)** Study the existence and uniqueness, non-negativeness, boundedness of the solution to system (4). **(ii)** Investigate the stability and the existence Hopf bifurcation of system (4). **(iii)** Adjust the stability domain and the emergence of Hopf bifurcation of system (4) by virtue of two extended hybrid controllers.

The major highlights of this study are summarized as follows: **(1)** A delay-independent Hopf bifurcation and stability condition for system (4) is built. **(2)** Taking advantage of two extended hybrid controllers, the time of emergence of Hopf bifurcation and stability domain of system (4) are effectively adjusted. **(3)** The role of delay in stabilizing system and controlling bifurcation of system (4) is explored.

This article is planned as follows. The properties of solution including non-negativeness, existence and uniqueness, boundedness of the solution yo system (4) are analyzed in Sect. 2. The Hopf bifurcation and stability of system (4) are investigated in Sect. 3. Sect. 4 is concerned with the control of Hopf bifurcation of system (4) by applying a suitable extended hybrid controller involving mixed controller (include state feedback and parameter perturbation with delay) and PD controller. Sect. 5. focuses on the control of Hopf bifurcation of system (4) by using a proper extended hybrid controller involving nonlinear delayed feedback controller and PD controller. Sect. 6. gives the related software simulation plots to verify the key acquired outcomes. Sect. 7 ends this work with a conclusion.

2 Property of solution

In this section, we are going to prove the existence and uniqueness, non-negativeness, boundedness of the solution of system (4) by using fixed point theorem, inequality skills and construction of function.

Theorem 2.1. *Let* $\Xi = \{w_1, w_2) \in R^2 : \max\{|w_1|, |w_2||\} \leq \mathcal{W}\}$*, where* $\mathcal{W}$ *is a positive constant. For every* $(w_{10}, w_{20}) \in \Xi$*, system (4) owing the initial value* (w_{10}, w_{20}) *has a unique solution* $W = (w_1, w_2) \in \Xi$*.*

Proof Define the following mapping:

$$\Gamma(W) = (\Gamma_1(W), \Gamma_2(W)), \tag{6}$$

where

$$\begin{cases} \Gamma_1(W) = qw_{10} - qw_1(t) - \dfrac{uw_1(t)w_2(t)}{(\kappa + w_1(t))(r + bw_1(t))}, \\ \Gamma_2(W) = -qw_2(t) + \dfrac{uw_1(t-\vartheta)w_2(t-\vartheta)}{\kappa + w_1(t-\vartheta)}. \end{cases} \tag{7}$$

For every $W, \tilde{W} \in \Xi$, one gains

$$\begin{aligned} & ||\Gamma(W) - \Gamma(\tilde{W})|| \\ & = \bigg| qw_{10} - qw_1(t) - \frac{uw_1(t)w_2(t)}{(\kappa + w_1(t))(r + bw_1(t))} \\ & \quad - \left[qw_{10} - q\tilde{w}_1(t) - \frac{u\tilde{w}_1(t)\tilde{w}_2(t)}{(\kappa + \tilde{w}_1(t))(r + b\tilde{w}_1(t))} \right] \bigg| \\ & \quad + \bigg| -qw_2(t) + \frac{uw_1(t-\vartheta)w_2(t-\vartheta)}{\kappa + w_1(t-\vartheta)} \\ & \quad - \left[-q\tilde{w}_2(t) + \frac{u\tilde{w}_1(t-\vartheta)\tilde{w}_2(t-\vartheta)}{\kappa + \tilde{w}_1(t-\vartheta)} \right] \bigg| \\ & \leq q|w_1(t) - \tilde{w}_1(t)| + u\mathcal{W}|w_1(t) - \tilde{w}_1(t)| + u\mathcal{W}|w_2(t) - \tilde{w}_2(t)| \\ & \quad + \frac{u(r + \kappa b)}{\kappa r}|w_2(t) - \tilde{w}_2(t)| + \frac{b\mathcal{W}^3}{\kappa r}|w_2(t) - \tilde{w}_2(t)| \\ & \quad + \frac{b\mathcal{W}^3}{\kappa r}|w_1(t) - \tilde{w}_1(t)| + q|w_2(t) - \tilde{w}_2(t)| \\ & \quad + \frac{u\mathcal{W}}{\kappa}|w_1(t-\vartheta) - \tilde{w}_1(t-\vartheta)| + \frac{u\mathcal{W}}{\kappa}|w_2(t-\vartheta) - \tilde{w}_2(t-\vartheta)| \\ & \leq \left(q + u\mathcal{W} + \frac{u\mathcal{W}}{\kappa} + \frac{b\mathcal{W}^3}{\kappa r} \right) |w_1(t) - \tilde{w}_1(t)| \\ & \quad + \left(q + u\mathcal{W} + \frac{u\mathcal{W}}{\kappa} + \frac{b\mathcal{W}^3}{\kappa r} + \frac{u(r + \kappa b)}{\kappa r} \right) |w_2(t) - \tilde{w}_2(t)| \\ & \leq \theta ||W - \tilde{W}||, \end{aligned} \tag{8}$$

where

$$\theta = q + u\mathcal{W} + \frac{u\mathcal{W}}{\kappa} + \frac{b\mathcal{W}^3}{\kappa r} + \frac{u(r + \kappa b)}{\kappa r}. \tag{9}$$

Then $\Gamma(W)$ obeys Lipschitz condition with respect to W (see [21]). Using fixed point theorem, we can easily know that Theorem 2.1 holds. ■

Theorem 2.2. *Suppose that $\vartheta = 0$, then every solution to system (4) beginning with R_+^2 is non-negative.*

Proof Let $W(t_0) = (w_1(t_0), w_2(t_0))$ be the initial condition of system (4). If there exists a constant $t_{00} > 0$ obeying $t_0 < t < t_{00}$ such that

$$\begin{cases} w_1(t) > 0, t_0 < t < t_{00}, \\ w_1(t_{00}) = 0, \\ w_1(t_{00}^+) < 0. \end{cases} \tag{10}$$

In view of system (4), one gets

$$\frac{dw_1(t)}{dt}|_{w_1(t_{00})=0} = qw_{10} > 0. \tag{11}$$

Using Lemma 1 of Das et al. [22], we understand that $w_1(t_{00}^+) = 0$, which is a contradiction (see (10)). Then $w_1(t) \geq 0$ for $t \geq t_0$. In a same way, one can lightly know that $w_2(t) \geq 0$ for $t \geq t_0$. ■

Theorem 2.3. *Suppose that $\vartheta = 0$ and $q > u$, then every solution to system (4) beginning with R_+^2 is uniformly bounded.*

Proof Define the function as follows:

$$V(t) = w_1(t) + w_2(t). \tag{12}$$

Then

$$\begin{aligned} \frac{dV(t)}{dt} &= \frac{dw_1(t)}{dt} + \frac{dw_2(t)}{dt} \\ &= qw_{10} - qw_1(t) - \frac{uw_1(t)w_2(t)}{(\kappa + w_1(t))(r + bw_1(t))} \\ & \quad -qw_2(t) + \frac{uw_1(t)w_2(t)}{\kappa + w_1(t)} \\ &\leq qw_{10} - qw_1(t) - qw_2(t) + \frac{uw_1(t)w_2(t)}{\kappa + w_1(t)} \\ &\leq qw_{10} - qw_1(t) - qw_2(t) + uw_2(t) \\ &\leq qw_{10} - qw_1(t) - (q-u)w_2(t) \\ &\leq -(q-u)V(t) + qw_{10}. \end{aligned} \tag{13}$$

By virtue of Gronwall's inequality [23], we gain

$$V(t) \to \frac{qw_{10}}{q-u}, \text{as } t \to \infty. \tag{14}$$

The proof of Theorem 2.3 ends. ∎

3 Exploration on bifurcation

Let $W(w_{1*}, w_{2*})$ be the equilibrium point of system (4). Then w_{1*}, w_{2*} satisfy

$$\begin{cases} qw_{10} - qw_{1*} - \dfrac{uw_{1*}w_{2*}}{(\kappa + w_{1*})(r + bw_{1*})} = 0, \\ -qw_{2*} + \dfrac{uw_{1*}w_{2*}}{\kappa + w_{1*}} = 0. \end{cases} \tag{15}$$

The linear system of model (4) at $W(w_{1*}, w_{2*})$ is given by

$$\begin{cases} \dfrac{dw_1(t)}{dt} = a_1 w_1(t) + a_2 w_2(t), \\ \dfrac{dw_2(t)}{dt} = a_3 w_2(t) + a_4 w_1(t-\vartheta) + a_5 w_2(t-\vartheta), \end{cases} \tag{16}$$

where

$$\begin{cases} a_1 = \dfrac{uw_{2*}}{(b + w_{1*})(r + bw_{1*})} - \dfrac{w_{1*}w_{2*}(b\kappa + bw_{1*} + r}{(b + w_{1*})^2(r + bw_{1*})^2} - q, \\ a_2 = \dfrac{uw_{1*}}{(b + w_{1*})(r + bw_{1*})}, \\ a_3 = -q, \\ a_4 = \dfrac{uw_{1*}w_{2*}}{\kappa} - \dfrac{uw_{1*}w_{2*}}{\kappa^2}, \\ a_5 = \dfrac{u}{\kappa}. \end{cases} \tag{17}$$

The characteristic equation of system (16) reads as

$$\det \begin{bmatrix} \lambda - a_1 & -a_2 \\ -a_4 e^{-\lambda\vartheta} & \lambda - a_3 - a_5 e^{-\lambda\vartheta} \end{bmatrix} = 0, \tag{18}$$

which leads to

$$\lambda^2 + b_1\lambda + b_2 + (b_3\lambda + b_4)e^{-\lambda\vartheta} = 0, \tag{19}$$

where

$$\begin{cases} b_1 = -(a_1 + a_3), \\ b_2 = a_1 a_3, \\ b_3 = -a_5, \\ b_4 = a_1 a_5 - a_2 a_5. \end{cases} \tag{20}$$

If $\vartheta = 0$, then Eq.(19) becomes

$$\lambda^2 + (b_1 + b_3)\lambda + b_2 + b_4 = 0. \tag{21}$$

If

$$(\mathcal{U}_1)\ b_1 + b_3 > 0, b_2 + b_4 > 0$$

holds, then the both roots λ_1, λ_2 of Eq. (21) admit negative real parts. Then the positive equilibrium point $W(w_{1*}, w_{2*})$ of model (4) concerning $\vartheta = 0$ maintains locally asymptotically stable situation.

Let $\lambda = i\epsilon$ be the root of Eq. (19). Then Eq.(19) owns the following form:

$$i\epsilon^2 + b_1 i\epsilon + b_2 + (b_3 i\phi + b_4)e^{-i\epsilon\vartheta} = 0, \tag{22}$$

which generates

$$-\epsilon^2 + ib_1\epsilon + b_2 + (b_3 i\epsilon + b_4)(\cos\epsilon\vartheta - i\sin\epsilon\vartheta) = 0. \tag{23}$$

In view of (23), one gains

$$\begin{cases} b_4\cos\epsilon\vartheta + b_3\epsilon\sin\epsilon\vartheta = \epsilon^2 - b_2, \\ b_3\epsilon\cos\epsilon\vartheta - b_4\sin\epsilon\vartheta = -b_1\epsilon. \end{cases} \tag{24}$$

By (24), one has

$$b_4^2 + (b_3\epsilon)^2 = (\epsilon^2 - b_2)^2 + (b_1\epsilon)^2, \tag{25}$$

which results in

$$\epsilon^4 + (b_1^2 - 2b_2 - b_3^2)\epsilon^2 + b_2^2 - b_4^2 = 0. \tag{26}$$

Let

$$\Delta_1(\epsilon) = \epsilon^4 + (b_1^2 - 2b_2 - b_3^2)\epsilon^2 + b_2^2 - b_4^2. \tag{27}$$

Suppose that

$$(\mathcal{U}_2)\ |b_2| < |b_4|$$

is met, since $\lim_{\epsilon\to+\infty} \Delta_1(\epsilon) = +\infty > 0$, then one understands that Eq. (26) admits at least one real positive root. Then Eq. (19) admits at least one couple of purely roots. Without loss of generality, here we assume that Eq. (26) owns four real positive roots (say $\epsilon_l, l = 1, 2, 3, 4$). By virtue of (24), one has

$$\vartheta_l^{(k)} = \frac{1}{\epsilon_l}\left[\arccos\left(\frac{(b_4 - b_1 b_3)\epsilon_l^2 - b_2 b_4}{b_4^2 + b_3\epsilon_l^2}\right) + 2k\pi\right], \tag{28}$$

where $l = 1, 2, 3, 4; k = 0, 1, 2, \cdots$. Denote $\vartheta_0 = \min_{\{l=1,2,3,4;k=0,1,2,\cdots\}}\{\vartheta_l^{(k)}\}$ and suppose that when $\vartheta = \vartheta_0$, (19) owns a couple of imaginary roots $\pm i\vartheta_0$. Next we prepare the assumption as follows:

$$(\mathcal{U}_3)\quad \mathcal{L}_{1R}\mathcal{L}_{2R} + \mathcal{L}_{1I}\mathcal{L}_{2I} > 0,$$

where

$$\begin{cases} \mathcal{L}_{1R} = b_1 + b_3\cos\epsilon_0\vartheta_0, \\ \mathcal{L}_{1I} = 2\epsilon_0 - b_3\sin\epsilon_0\vartheta_0, \\ \mathcal{L}_{2R} = b_4\epsilon_0\sin\epsilon_0\vartheta_0 - b_3\epsilon_0\cos\epsilon_0\vartheta_0, \\ \mathcal{L}_{2I} = b_4\epsilon_0\cos\epsilon_0\vartheta_0 + b_3\epsilon_0\sin\epsilon_0\vartheta_0. \end{cases} \tag{29}$$

Lemma 3.1. *Denote $\lambda(\vartheta) = s_1(\vartheta) + is_2(\vartheta)$ the root of Eq. (19) at $\vartheta = \vartheta_0$ obeying $s_1(\vartheta_0) = 0, s_2(\vartheta_0) = \epsilon_0$, then Re $\left(\frac{d\lambda}{d\vartheta}\right)\Big|_{\vartheta=\vartheta_0,\epsilon=\epsilon_0} > 0$.*

Proof By virtue of Eq.(19), one gets

$$2\lambda\frac{d\lambda}{d\vartheta} + b_1\frac{d\lambda}{d\vartheta} + b_3\frac{d\lambda}{d\vartheta}e^{-\lambda\vartheta} - e^{-\lambda\vartheta}(b_3\lambda + b_4)\left(\frac{d\lambda}{d\vartheta}\vartheta + \lambda\right) = 0, \tag{30}$$

which implies

$$\left(\frac{d\lambda}{d\rho}\right)^{-1} = \frac{\mathcal{L}_1(\lambda)}{\mathcal{L}_2(\lambda)} - \frac{\rho}{\lambda}, \tag{31}$$

where

$$\begin{cases} \mathcal{L}_1(\lambda) = 2\lambda + b_1 + b_3 e^{-\lambda\vartheta}, \\ \mathcal{L}_2(\lambda) = \lambda(b_3\lambda + b_4)e^{-\lambda\vartheta}. \end{cases} \tag{32}$$

Hence

$$\text{Re}\left[\left(\frac{d\lambda}{d\vartheta}\right)^{-1}\right]_{\vartheta=\vartheta_0,\epsilon=\epsilon_0} = \text{Re}\left[\frac{\mathcal{L}_1(\lambda)}{\mathcal{L}_2(\lambda)}\right]_{\vartheta=\vartheta_0,\epsilon=\epsilon_0} = \frac{\mathcal{L}_{1R}\mathcal{L}_{2R} + \mathcal{L}_{1I}\mathcal{L}_{2I}}{\mathcal{L}_{2R}^2 + \mathcal{L}_{2I}^2}. \tag{33}$$

Using $(\mathcal{U}_3)$, one gains

$$\text{Re}\left[\left(\frac{d\lambda}{d\vartheta}\right)^{-1}\right]_{\vartheta=\vartheta_0,\epsilon=\epsilon_0} > 0. \tag{34}$$

The proof finishes. ■

Relying on the exploration above, the following outcomes can be easily acquired.

Theorem 3.1. *If* $(\mathcal{U}_1)$-$(\mathcal{U}_3)$ *hold true, then the positive equilibrium point* $W(w_{1*}, w_{2*})$ *of model (4) keeps locally asymptotically stable state if* $\vartheta \in [0, \vartheta_0)$ *and model (4) produces a cluster of Hopf bifurcations near the positive equilibrium point* $W(w_{1*}, w_{2*})$ *when* $\vartheta = \vartheta_0$.

4 Bifurcation control via extended hybrid controller I

In this section, we are going to explore the control problem of Hopf bifurcation in system (4) by virtue of a suitable extended hybrid controller (include a PD controller and a mixed controller owing parameter perturbation involving delay and state feedback. By virtue of the work of [24–28], the following controlled delayed chemostat model is acquired:

$$\begin{cases} \dfrac{dw_1(t)}{dt} = \tau_1 \left[qw_{10} - qw_1(t) - \dfrac{uw_1(t)w_2(t)}{(\kappa + w_1(t))(r + bw_1(t))} \right] \\ \qquad\qquad + \tau_2[w_1(t-\vartheta) - w_1(t)], \\ \dfrac{dw_2(t)}{dt} = -qw_2(t) + \dfrac{uw_1(t-\vartheta)w_2(t-\vartheta)}{\kappa + w_1(t-\vartheta)} \\ \qquad\qquad + \rho_p[w_2(t) - w_{2*}] + \rho_d \dfrac{d(w_2(t) - w_{2*})}{dt}, \end{cases} \tag{35}$$

where τ_1, τ_2 are feedback gain parameters and $\rho_p, \rho_d \neq 1$ are the proportional control parameter and the derivative control parameter, respectively. Clearly, system (35) and system (4) admit the identical equilibrium points $W(w_{1*}, w_{2*})$. The linear system of system (35) near $W(w_{1*}, w_{2*})$ reads as

$$\begin{cases} \dfrac{dw_1(t)}{dt} = c_1 w_1(t) + c_2 w_2(t) + c_3 w_1(t-\vartheta), \\ \dfrac{dw_2(t)}{dt} = c_4 w_2(t) + c_5 w_1(t-\vartheta) + c_6 w_2(t-\vartheta), \end{cases} \tag{36}$$

where

$$\begin{cases} c_1 = \tau_1 \left[\dfrac{uw_{2*}}{(b + w_{1*})(r + bw_{1*})} - \dfrac{w_{1*}w_{2*}(b\kappa + bw_{1*} + r}{(b + w_{1*})^2(r + bw_{1*})^2} - q \right] - \tau_2, \\ c_2 = \dfrac{\tau_1 uw_{1*}}{(b + w_{1*})(r + bw_{1*})}, \\ c_3 = \tau_2, \\ c_4 = \dfrac{\rho_p - q}{1 - \rho_d}, \\ c_5 = \dfrac{uw_{1*}w_{2*}}{\kappa(1 - \rho_d)} - \dfrac{uw_{1*}w_{2*}}{\kappa^2(1 - \rho_d)}, \\ c_6 = \dfrac{u}{\kappa(1 - \rho_d)}. \end{cases} \tag{37}$$

The characteristic equation of system (36) reads as

$$\det \begin{bmatrix} \lambda - c_1 - c_3 e^{-\lambda\vartheta} & -c_2 \\ -c_5 e^{-\lambda\vartheta} & \lambda - c_4 - c_6 e^{-\lambda\vartheta} \end{bmatrix} = 0, \tag{38}$$

which leads to

$$\lambda^2 + d_1\lambda + d_2 + (d_3\lambda + d_4)e^{-\lambda\vartheta} + d_5 e^{-2\lambda\vartheta} = 0, \tag{39}$$

where

$$\begin{cases} d_1 = -(c_1 + c_4), \\ d_2 = c_1 c_4, \\ d_3 = -(c_3 + c_6), \\ d_4 = c_1 c_6 - c_2 c_5 + c_3 c_4, \\ d_5 = c_3 c_6. \end{cases} \tag{40}$$

It follows from (39) that

$$(\lambda^2 + d_1\lambda + d_2)e^{\lambda\vartheta} + (d_3\lambda + d_4) + d_5 e^{-\lambda\vartheta} = 0. \tag{41}$$

If $\vartheta = 0$, then Eq.(39) becomes

$$\lambda^2 + (d_1 + d_3)\lambda + d_2 + d_4 + d_5 = 0. \tag{42}$$

If

$$(\mathcal{U}_4)\ d_1 + d_3 > 0, d_2 + d_4 + d_5 > 0$$

holds, then the both roots λ_1, λ_2 of Eq. (42) admit negative real parts. Then the positive equilibrium point $W(w_{1*}, w_{2*})$ of model (35) concerning $\vartheta = 0$ maintains locally asymptotically stable situation.

Let $\lambda = i\varepsilon$ be the root of Eq. (41). Then Eq.(41) owns the following form:

$$[(i\varepsilon)^2 + d_1 i\varepsilon + d_2]e^{i\varepsilon\vartheta} + (d_3 i\varepsilon + d_4) + d_5 e^{-i\varepsilon\vartheta} = 0, \tag{43}$$

which generates

$$(-\varepsilon^2 + d_1 i\varepsilon + d_2)(\cos\varepsilon\vartheta + i\sin\varepsilon\vartheta) + (d_3 i\varepsilon + d_4) + d_5(\cos\varepsilon\vartheta - i\sin\varepsilon\vartheta) = 0. \tag{44}$$

In view of (44), one gains

$$\begin{cases} (d_2 - \varepsilon^2 + d_5)\cos\varepsilon\vartheta - d_1\varepsilon\sin\varepsilon\vartheta = -d_4, \\ d_1\varepsilon\cos\varepsilon\vartheta + (d_2 - \varepsilon^2 - d_5)\sin\varepsilon\vartheta = -d_3\varepsilon. \end{cases} \tag{45}$$

By (45), one has

$$\begin{cases} \cos\varepsilon\vartheta = \dfrac{(d_4 - d_1 d_3)\varepsilon^2 + d_4 d_5 - d_2 d_4}{\varepsilon^4 + (d_1^2 - 2d_2)\varepsilon^2 + d_2^2 - d_5^2}, \\ \sin\varepsilon\vartheta = \dfrac{d_1\varepsilon^3 + (d_2 d_3 - d_1 d_4 - d_3 d_5)\varepsilon}{\varepsilon^4 + (d_1^2 - 2d_2)\varepsilon^2 + d_2^2 - d_5^2}. \end{cases} \tag{46}$$

In view of $\cos^2\varepsilon\vartheta + \sin^2\varepsilon\vartheta = 1$, it follows from (46) that

$$\begin{aligned} &[(d_4 - d_1 d_3)\varepsilon^2 + d_4 d_5 - d_2 d_4]^2 + [d_1\varepsilon^3 + (d_2 d_3 - d_1 d_4 - d_3 d_5)\varepsilon]^2 \\ &= [\varepsilon^4 + (d_1^2 - 2d_2)\varepsilon^2 + d_2^2 - d_5^2]^2, \end{aligned} \tag{47}$$

which results in

$$\varepsilon^8 + \nu_1\varepsilon^6 + \nu_2\varepsilon^4 + \nu_3\varepsilon^2 + \nu_4 = 0. \tag{48}$$

where

$$\begin{cases} \nu_1 = 2(d_1^2 - 2d_2) - d_1^2, \\ \nu_2 = (d_1^2 - 2d_2)^2 + 2(d_2^2 - d_5^2) - (d_4 - d_1 d_3)^2 \\ \qquad - 2d_1(d_2 d_3 - d_1 d_4 - d_3 d_5), \\ \nu_3 = 2(d_1^2 - 2d_2)(d_2^2 - d_5^2) - 2(d_4 - d_1 d_3)(d_4 d_5 - d_2 d_4) \\ \qquad - (d_2 d_3 - d_1 d_4 - d_3 d_5)^2, \\ \nu_4 = (d_2^2 - d_5^2)^2 - (d_4 d_5 - d_2 d_4)^2. \end{cases} \tag{49}$$

Let

$$\Delta_2(\varepsilon) = \varepsilon^8 + \nu_1\varepsilon^6 + \nu_2\varepsilon^4 + \nu_3\varepsilon^2 + \nu_4. \tag{50}$$

Suppose that

$$(\mathcal{U}_5)\ |d_2^2 - d_5^2| < |d_4 d_5 - d_2 d_4|$$

is met, since $\lim_{\varepsilon\to+\infty}\Delta_2(\varepsilon)=+\infty>0$, then one understands that Eq. (48) admits at least one real positive root. Then Eq. (39) admits at least one couple of purely roots. Without loss of generality, here we assume that Eq. (48) owns eight real positive roots (say $\varepsilon_i, i=1,2,\cdots,8$). By virtue of (46), one has

$$\vartheta_i^{(k)}=\frac{1}{\varepsilon_i}\left[\arccos\left(\frac{(d_4-d_1d_3)\varepsilon_i^2+d_4d_5-d_2d_4}{\varepsilon_i^4+(d_1^2-2d_2)\varepsilon_i^2+d_2^2-d_5^2}\right)+2k\pi\right], \tag{51}$$

where $i=1,2,\cdots,8; k=0,1,2,\cdots$. Denote

$$\vartheta_*=\min_{\{i=1,2,\cdots,8;k=0,1,2,\cdots\}}\{\vartheta_i^{(k)}\}$$

and suppose that when $\vartheta=\vartheta_*$, (39) owns a couple of imaginary roots $\pm i\vartheta_*$.

Next we prepare the assumption as follows:

$$(\mathcal{U}_6)\quad \mathcal{H}_{1R}\mathcal{H}_{2R}+\mathcal{H}_{1I}\mathcal{H}_{2I}>0,$$

where

$$\begin{cases}\mathcal{H}_{1R}=d_1+d_3\cos\varepsilon_0\vartheta_*,\\ \mathcal{H}_{1I}=2\varepsilon_0-d_3\sin\varepsilon_0\vartheta_*,\\ \mathcal{H}_{2R}=d_4\varepsilon_0\sin\varepsilon_0\vartheta_*-d_3\varepsilon_0\cos\varepsilon_0\vartheta_*+2d_5\varepsilon_0\sin 2\varepsilon_0\vartheta_*,\\ \mathcal{H}_{2I}=d_4\varepsilon_0\cos\varepsilon_0\vartheta_*+d_3\varepsilon_0\sin\varepsilon_0\vartheta_*-2d_5\varepsilon_0\cos 2\varepsilon_0\vartheta_*.\end{cases} \tag{52}$$

Lemma 4.1. *Denote $\lambda(\vartheta)=\gamma_1(\vartheta)+i\gamma_2(\vartheta)$ the root of Eq. (39) at $\vartheta=\vartheta_*$ obeying $\gamma_1(\vartheta_*)=0, \gamma_2(\vartheta_*)=\varepsilon_0$, then Re $\left(\frac{d\lambda}{d\vartheta}\right)\Big|_{\vartheta=\vartheta_*,\epsilon=\epsilon_*}>0$.*

Proof By virtue of Eq.(39), one gets

$$\begin{aligned}&(2\lambda+d_1)\frac{d\lambda}{d\vartheta}+d_3\frac{d\lambda}{d\vartheta}e^{-\lambda\vartheta}-e^{-\lambda\vartheta}(d_3\lambda+d_4)\\ &\times\left(\frac{d\lambda}{d\vartheta}\vartheta+\lambda\right)-2d_5e^{-2\lambda\vartheta}\left(\frac{d\lambda}{d\vartheta}\vartheta+\lambda\right)=0,\end{aligned} \tag{53}$$

which implies

$$\left(\frac{d\lambda}{d\vartheta}\right)^{-1}=\frac{\mathcal{H}_1(\lambda)}{\mathcal{H}_2(\lambda)}-\frac{\vartheta}{\lambda}, \tag{54}$$

where

$$\begin{cases}\mathcal{H}_1(\lambda)=2\lambda+d_1+d_3e^{-\lambda\vartheta},\\ \mathcal{H}_2(\lambda)=\lambda(d_3\lambda+d_4)e^{-\lambda\vartheta}+2d_5\lambda e^{-2\lambda\vartheta}.\end{cases} \tag{55}$$

Hence

$$\text{Re}\left[\left(\frac{d\lambda}{d\vartheta}\right)^{-1}\right]_{\vartheta=\vartheta_*,\epsilon=\epsilon_*}=\text{Re}\left[\frac{\mathcal{H}_1(\lambda)}{\mathcal{H}_2(\lambda)}\right]_{\vartheta=\vartheta_*,\epsilon=\epsilon_*}=\frac{\mathcal{H}_{1R}\mathcal{H}_{2R}+\mathcal{H}_{1I}\mathcal{H}_{2I}}{\mathcal{H}_{2R}^2+\mathcal{H}_{2I}^2}. \tag{56}$$

Using $(\mathcal{U}_6)$, one gains

$$\text{Re}\left[\left(\frac{d\lambda}{d\vartheta}\right)^{-1}\right]_{\vartheta=\vartheta_*,\epsilon=\epsilon_*}>0. \tag{57}$$

The proof finishes. ■

Relying on the exploration above, the following outcomes can be easily acquired.

Theorem 4.1. *If $(\mathcal{U}_4)$-$(\mathcal{U}_6)$ hold true, then the positive equilibrium point $W(w_{1*},w_{2*})$ of model (35) keeps locally asymptotically stable state if $\vartheta\in[0,\vartheta_*)$ and model (35) produces a cluster of Hopf bifurcations near the positive equilibrium point $W(w_{1*},w_{2*})$ when $\vartheta=\vartheta_*$.*

5 Bifurcation control via extended hybrid controller II

In this section, we are going to explore the control problem of Hopf bifurcation in system (4) by virtue of a suitable extended hybrid controller (include a PD controller and a nonlinear delayed feedback controller. By virtue of the work of [28, 29], the following controlled delayed chemostat model is acquired:

$$\begin{cases} \dfrac{dw_1(t)}{dt} = qw_{10} - qw_1(t) - \dfrac{uw_1(t)w_2(t)}{(\kappa + w_1(t))(r + bw_1(t))} \\ \qquad\qquad + \xi_1[w_1(t-\vartheta) - w_1(t)] + \xi_2[w_1(t-\vartheta) - w_1(t)]^2, \\ \dfrac{dw_2(t)}{dt} = -qw_2(t) + \dfrac{uw_1(t-\vartheta)w_2(t-\vartheta)}{\kappa + w_1(t-\vartheta)} \\ \qquad\qquad + \mu_p[w_2(t) - w_{2*}] + \mu_d \dfrac{d(w_2(t) - w_{2*})}{dt}, \end{cases} \tag{58}$$

where ξ_1, ξ_2 are feedback gain parameters and $\mu_p, \mu_d \neq 1$ are the proportional control parameter and the derivative control parameter, respectively. Clearly, system (58) and system (4) admit the identical equilibrium points $W(w_{1*}, w_{2*})$. The linear system of system (58) near $W(w_{1*}, w_{2*})$ reads as

$$\begin{cases} \dfrac{dw_1(t)}{dt} = e_1w_1(t) + e_2w_2(t) + e_3w_1(t-\vartheta), \\ \dfrac{dw_2(t)}{dt} = e_4w_2(t) + e_5w_1(t-\vartheta) + e_6w_2(t-\vartheta), \end{cases} \tag{59}$$

where

$$\begin{cases} e_1 = \dfrac{uw_{2*}}{(b + w_{1*})(r + bw_{1*})} - \dfrac{w_{1*}w_{2*}(b\kappa + bw_{1*} + r}{(b + w_{1*})^2(r + bw_{1*})^2} - q - \xi_1, \\ e_2 = \dfrac{uw_{1*}}{(b + w_{1*})(r + bw_{1*})}, \\ e_3 = \xi_1, \\ e_4 = \dfrac{\rho_p - q}{1 - \mu_d}, \\ e_5 = \dfrac{uw_{1*}w_{2*}}{\kappa(1 - \rho_d)} - \dfrac{uw_{1*}w_{2*}}{\kappa^2(1 - \mu_d)}, \\ e_6 = \dfrac{u}{\kappa(1 - \mu_d)}. \end{cases} \tag{60}$$

The characteristic equation of system (59) owns the following expression:

$$\det \begin{bmatrix} \lambda - e_1 - e_3e^{-\lambda\vartheta} & -e_2 \\ -e_5e^{-\lambda\vartheta} & \lambda - e_4 - e_6e^{-\lambda\vartheta} \end{bmatrix} = 0, \tag{61}$$

which leads to

$$\lambda^2 + f_1\lambda + f_2 + (f_3\lambda + f_4)e^{-\lambda\vartheta} + f_5 e^{-2\lambda\vartheta} = 0, \tag{62}$$

where

$$\begin{cases} f_1 = -(e_1 + e_4), \\ f_2 = e_1 e_4, \\ f_3 = -(e_3 + e_6), \\ f_4 = e_1 e_6 - e_2 e_5 + e_3 e_4, \\ f_5 = e_3 e_6. \end{cases} \tag{63}$$

It follows from (62) that

$$(\lambda^2 + f_1\lambda + f_2)e^{\lambda\vartheta} + (f_3\lambda + f_4) + f_5 e^{-\lambda\vartheta} = 0. \tag{64}$$

If $\vartheta = 0$, then Eq.(62) becomes

$$\lambda^2 + (f_1 + f_3)\lambda + f_2 + f_4 + f_5 = 0. \tag{65}$$

If

$$(\mathcal{U}_7)\ f_1 + f_3 > 0, f_2 + f_4 + f_5 > 0$$

holds, then the both roots λ_1, λ_2 of Eq. (64) admit negative real parts. Then the positive equilibrium point w_{1*}, w_{2*} of model (58) concerning $\vartheta = 0$ maintains locally asymptotically stable situation.

Let $\lambda = i\zeta$ be the root of Eq. (64). Then Eq.(64) owns the following form:

$$[(i\zeta)^2 + f_1 i\zeta + f_2]e^{i\zeta\vartheta} + (f_3 i\zeta + f_4) + f_5 e^{-i\zeta\vartheta} = 0, \tag{66}$$

which generates

$$(-\zeta^2 + f_1 i\zeta + f_2)(\cos\zeta\vartheta + i\sin\zeta\vartheta) + (f_3 i\zeta + f_4) + f_5(\cos\zeta\vartheta - i\sin\zeta\vartheta) = 0. \tag{67}$$

In view of (67), one gains

$$\begin{cases} (f_2-\zeta^2+d_5)\cos\sigma\vartheta - f_1\zeta\sin\zeta\vartheta = -f_4, \\ f_1\zeta\cos\zeta\vartheta + (f_2-\zeta^2-f_5)\sin\zeta\vartheta = -f_3\zeta. \end{cases} \tag{68}$$

By (68), one has

$$\begin{cases} \cos\zeta\vartheta = \dfrac{(f_4-f_1f_3)\zeta^2+f_4f_5-f_2f_4}{\zeta^4+(f_1^2-2f_2)\zeta^2+f_2^2-f_5^2}, \\ \sin\zeta\vartheta = \dfrac{f_1\zeta^3+(f_2f_3-f_1f_4-f_3f_5)\zeta}{\zeta^4+(f_1^2-2f_2)\zeta^2+f_2^2-f_5^2}. \end{cases} \tag{69}$$

In view of $\cos^2\zeta\vartheta+\sin^2\zeta\vartheta=1$, it follows from (69) that

$$\begin{aligned} &[(f_4-f_1f_3)\zeta^2+f_4f_5-f_2f_4]^2+[f_1\zeta^3+(f_2f_3-f_1f_4-f_3f_5)\zeta]^2 \\ &=[\zeta^4+(f_1^2-2f_2)\zeta^2+f_2^2-f_5^2]^2, \end{aligned} \tag{70}$$

which results in

$$\zeta^8+\eta_1\zeta^6+\eta_2\zeta^4+\eta_3\zeta^2+\eta_4=0. \tag{71}$$

where

$$\begin{cases} \eta_1 = 2(f_1^2-2f_2)-f_1^2, \\ \eta_2 = (f_1^2-2f_2)^2+2(f_2^2-f_5^2)-(f_4-f_1f_3)^2 \\ \qquad -2f_1(f_2f_3-f_1f_4-f_3f_5), \\ \eta_3 = 2(f_1^2-2f_2)(f_2^2-f_5^2)-2(f_4-f_1f_3)(f_4f_5-f_2f_4) \\ \qquad -(f_2f_3-f_1f_4-f_3f_5)^2, \\ \eta_4 = (f_2^2-f_5^2)^2-(f_4f_5-f_2f_4)^2. \end{cases} \tag{72}$$

Let

$$\Delta_3(\zeta)=\zeta^8+\eta_1\zeta^6+\eta_2\zeta^4+\eta_3\zeta^2+\eta_4. \tag{73}$$

Suppose that

$$(\mathcal{U}_8)\ |f_2^2-f_5^2| < |f_4f_5-f_2f_4|$$

is met, since $\lim_{\zeta\to+\infty}\Delta_3(\zeta)=+\infty>0$, then one understands that Eq. (71) admits at least one real positive root. Then Eq. (62) admits at least one couple of purely roots. Without loss of generality, here we assume that Eq. (71) owns eight real positive roots (say $\zeta_i, i=1,2,\cdots,8$). By virtue of (69), one has

$$\vartheta_i^{(k)}=\frac{1}{\zeta_i}\left[\arccos\left(\frac{(f_4-f_1f_3)\zeta_i^2+f_4f_5-f_2f_4}{\zeta_i^4+(f_1^2-2f_2)\zeta_i^2+f_2^2-f_5^2}\right)+2k\pi\right], \qquad (74)$$

where $i=1,2,\cdots,8; k=0,1,2,\cdots$. Denote

$$\vartheta_{*0}=\min_{\{i=1,2,\cdots,8;k=0,1,2,\cdots\}}\{\vartheta_i^{(k)}\}$$

and suppose that when $\vartheta=\vartheta_{*0}$, (62) owns a couple of imaginary roots $\pm i\vartheta_{*0}$.

Next we prepare the assumption as follows:

$$(\mathcal{U}_9)\quad \mathcal{Q}_{1R}\mathcal{Q}_{2R}+\mathcal{Q}_{1I}\mathcal{Q}_{2I}>0,$$

where

$$\begin{cases}\mathcal{Q}_{1R}=f_1+f_3\cos\zeta_0\vartheta_{*0},\\ \mathcal{Q}_{1I}=2\zeta_0-f_3\sin\zeta_0\vartheta_{*0},\\ \mathcal{Q}_{2R}=f_4\zeta_0\sin\zeta_0\vartheta_{*0}-f_3\zeta_0\cos\zeta_0\vartheta_{*}+2f_5\zeta_0\sin2\zeta_0\vartheta_{*0},\\ \mathcal{Q}_{2I}=f_4\zeta_0\cos\zeta_0\vartheta_{*0}+f_3\zeta_0\sin\zeta_0\vartheta_{*0}-2f_5\zeta_0\cos2\zeta_0\vartheta_{*0}.\end{cases} \qquad (75)$$

Lemma 5.1. *Denote $\lambda(\vartheta)=\chi_1(\vartheta)+i\chi_2(\vartheta)$ the root of Eq. (62) at $\vartheta=\vartheta_{*0}$ obeying $\chi_1(\vartheta_{*0})=0, \chi_2(\vartheta_{*0})=\zeta_0$, then Re $\left(\frac{d\lambda}{d\vartheta}\right)\Big|_{\vartheta=\vartheta_{*0},\zeta=\zeta_0}>0$.*

Proof By virtue of Eq.(62), one gets

$$(2\lambda+f_1)\frac{d\lambda}{d\vartheta}+f_3\frac{d\lambda}{d\vartheta}e^{-\lambda\vartheta}-e^{-\lambda\vartheta}(f_3\lambda+f_4)\times\left(\frac{d\lambda}{d\vartheta}\vartheta+\lambda\right)-2f_5e^{-2\lambda\vartheta}\left(\frac{d\lambda}{d\vartheta}\vartheta+\lambda\right)=0, \qquad (76)$$

which implies

$$\left(\frac{d\lambda}{d\vartheta}\right)^{-1} = \frac{\mathcal{Q}_1(\lambda)}{\mathcal{Q}_2(\lambda)} - \frac{\vartheta}{\lambda}, \tag{77}$$

where

$$\begin{cases} \mathcal{Q}_1(\lambda) = 2\lambda + f_1 + f_3 e^{-\lambda\vartheta}, \\ \mathcal{Q}_2(\lambda) = \lambda(f_3\lambda + f_4)e^{-\lambda\vartheta} + 2f_5\lambda e^{-2\lambda\vartheta}. \end{cases} \tag{78}$$

Hence

$$\mathrm{Re}\left[\left(\frac{d\lambda}{d\vartheta}\right)^{-1}\right]_{\vartheta=\vartheta_{*0},\zeta=\zeta_0} = \mathrm{Re}\left[\frac{\mathcal{Q}_1(\lambda)}{\mathcal{Q}_2(\lambda)}\right]_{\vartheta=\vartheta_{*0},\zeta=\zeta_0} = \frac{\mathcal{Q}_{1R}\mathcal{Q}_{2R} + \mathcal{Q}_{1I}\mathcal{Q}_{2I}}{\mathcal{Q}_{2R}^2 + \mathcal{Q}_{2I}^2}. \tag{79}$$

Using $(\mathcal{U}_9)$, one gains

$$\mathrm{Re}\left[\left(\frac{d\lambda}{d\vartheta}\right)^{-1}\right]_{\vartheta=\vartheta_{*0},\zeta=\zeta_0} > 0. \tag{80}$$

The proof finishes. ■

Relying on the exploration above, the following outcomes can be easily acquired.

Theorem 5.1. *If $(\mathcal{U}_7)$-$(\mathcal{U}_9)$ hold true, then the positive equilibrium point $W(w_{1*}, w_{2*})$ of model (58) keeps locally asymptotically stable state if $\vartheta \in [0, \vartheta_{*0})$ and model (58) produces a cluster of Hopf bifurcations near the positive equilibrium point $W(w_{1*}, w_{2*})$ when $\vartheta = \vartheta_{*0}$.*

Remark 5.1. *In 2021, Mohd Aris and Jamaian [14] investigated the dynamics of the fractional-order delayed chemostat model (5). In this paper, We have explored the existence and uniqueness, non-negativeness and boundedness of the solution of the integer-order delayed chemostat model (4). Furthermore, we also explore the Hopf bifurcation and Hopf bifurcation control issue of integer-order delayed chemostat model (4) via stability and bifurcation control theory of fractional-order dynamical system. The obtained outcomes are completely new and supplement the work of Mohd Aris and Jamaian [14] to some degree.*

6 Software experiments

Example 6.1. Give the delayed chemostat model as follows:

$$\begin{cases} \dfrac{dw_1(t)}{dt} = qw_{10} - qw_1(t) - \dfrac{uw_1(t)w_2(t)}{(\kappa + w_1(t))(r + bw_1(t))}, \\ \dfrac{dw_2(t)}{dt} = -qw_2(t) + \dfrac{uw_1(t-\vartheta)w_2(t-\vartheta)}{\kappa + w_1(t-\vartheta)}, \end{cases} \tag{81}$$

where $q = 0.02, w_{10} = 1, u = 0.3, \kappa = 1.75, r = 0.01, b = 5.25$. One can lightly obtain that system (81) possesses the positive equilibrium point $W(0.1250, 0.5830)$. One can check that the hypotheses $(\mathcal{U}_1)$-$(\mathcal{U}_3)$ in Theorem 3.1 hold true. By virtue of software, one gains $\epsilon_0 = 1.5631, \vartheta_0 \approx 5.3$. To verify the correctness of the gained conclusions in Theorem 3.1, we will choose both distinct time delay values. Let $\vartheta = 4.5$ and $\vartheta = 6.5$. For $\vartheta = 4.5 < \vartheta_0 \approx 5.3$, the software simulation figures are given in Figures 1-4. According to Figures 1-4, we can easily determine that $w_1 \to 0.1250, w_2 \to 0.5830$ when $t \to +\infty$. In other word, the positive equilibrium point $W(0.1250, 0.5830)$ of system (81) preserves locally asymptotically stable situation. For $\vartheta = 6.5 > \vartheta_0 \approx 5.3$, the software simulation figures are given in Figures 5-8. According to Figures 5-8, we can easily determine that w_1 will preserve periodic oscillatory situation around the value 0.1250, w_2 will preserve periodic oscillatory situation around the value 0.5830. In other word, a cluster of limit cycles (namely, Hopf bifurcations) arise near the positive equilibrium point $W(0.1250, 0.5830)$.

Example 6.2. Give the controlled delayed chemostat model as follows:

$$\begin{cases} \dfrac{dw_1(t)}{dt} = \tau_1 \left[qw_{10} - qw_1(t) - \dfrac{uw_1(t)w_2(t)}{(\kappa + w_1(t))(r + bw_1(t))} \right] \\ \qquad\qquad + \tau_2[w_1(t-\vartheta) - w_1(t)], \\ \\ \dfrac{dw_2(t)}{dt} = -qw_2(t) + \dfrac{uw_1(t-\vartheta)w_2(t-\vartheta)}{\kappa + w_1(t-\vartheta)} \\ \qquad\qquad + \rho_p[w_2(t) - w_{2*}] + \rho_d \dfrac{d(w_2(t) - w_{2*})}{dt}, \end{cases} \tag{82}$$

where $q = 0.02, w_{10} = 1, u = 0.3, \kappa = 1.75, r = 0.01, b = 5.25$. Let $\tau_1 = 0.4, \tau_2 = 0.6, \rho_p = 0.3, \rho_d = 0.4$. One can lightly obtain that system (82) possesses the positive equilibrium point $W(0.1250, 0.5830)$. One can check that the hypotheses $(\mathcal{U}_1)$-$(\mathcal{U}_3)$ in Theorem 4.1 hold true. By virtue of software, one gains $\varepsilon_0 = 3.0923, \vartheta_* \approx 2.5$. To verify the correctness of the gained conclusions in Theorem 4.1, we will choose both distinct time delay values. Let $\vartheta = 2.1$ and $\vartheta = 3.5$. For $\vartheta = 2.1 < \vartheta_0 \approx 2.5$, the software simulation figures are given in Figures 9-12. According to Figures 9-12, we can easily determine that $w_1 \to 0.1250, w_2 \to 0.5830$ when $t \to +\infty$. In other word, the positive equilibrium point $W(0.1250, 0.5830)$ of system (82) preserves locally asymptotically stable situation. For $\vartheta = 3.5 > \vartheta_0 \approx 2.5$, the software simulation figures are given in Figures 13-16. According to Figures 13-16, we can easily determine that w_1 will preserve periodic oscillatory situation around the value 0.1250, w_2 will preserve periodic oscillatory situation around the value 0.5830. In other word, a cluster of limit cycles (namely, Hopf bifurcations) arise near the positive equilibrium point $W(0.1250, 0.5830)$.

Example 6.3. Give the controlled delayed chemostat model as follows:

$$\begin{cases} \dfrac{dw_1(t)}{dt} = qw_{10} - qw_1(t) - \dfrac{uw_1(t)w_2(t)}{(\kappa + w_1(t))(r + bw_1(t))} \\ \qquad + \xi_1[w_1(t-\vartheta) - w_1(t)] + \xi_2[w_1(t-\vartheta) - w_1(t)]^2, \\ \dfrac{dw_2(t)}{dt} = -qw_2(t) + \dfrac{uw_1(t-\vartheta)w_2(t-\vartheta)}{\kappa + w_1(t-\vartheta)} \\ \qquad + \mu_p[w_2(t) - w_{2*}] + \mu_d \dfrac{d(w_2(t) - w_{2*})}{dt}, \end{cases} \tag{83}$$

where $q = 0.02, w_{10} = 1, u = 0.3, \kappa = 1.75, r = 0.01, b = 5.25$. Let $\xi_1 = 0.2, \xi_2 = 0.4, \mu_p = 0.4, \mu_d = 0.2$. One can lightly obtain that system (83) possesses the positive equilibrium point $W(0.1250, 0.5830)$. One can check that the hypotheses $(\mathcal{U}_1)$-$(\mathcal{U}_3)$ in Theorem 5.1 hold true. By virtue of software, one gains $\zeta_0 = 2.0078, \vartheta_{*0} \approx 2.1$. To verify the correctness of the gained conclusions in Theorem 5.1, we will choose both distinct time delay values. Let $\vartheta = 1.98$ and $\vartheta = 2.25$. For $\vartheta = 1.98 < \vartheta_{*0} \approx 2.1$, the software simulation figures are given in Figures 17-20. According to Figures 17-20, we can easily determine that $w_1 \to 0.1250, w_2 \to 0.5830$ when $t \to +\infty$. In other word, the positive equilibrium point $W(0.1250, 0.5830)$ of system (83) preserves locally asymptotically stable situation. For $\vartheta = 2.25 > \vartheta_{*0} \approx 2.1$, the software simulation figures are given in Figures 21-24. According to Figures 21-24, we can easily determine that w_1 will preserve periodic oscillatory situation around the value 0.1250, w_2 will preserve periodic oscillatory situation around the value 0.5830. In other word, a cluster of limit cycles (namely, Hopf bifurcations) arise near the positive equilibrium point $W(0.1250, 0.5830)$.

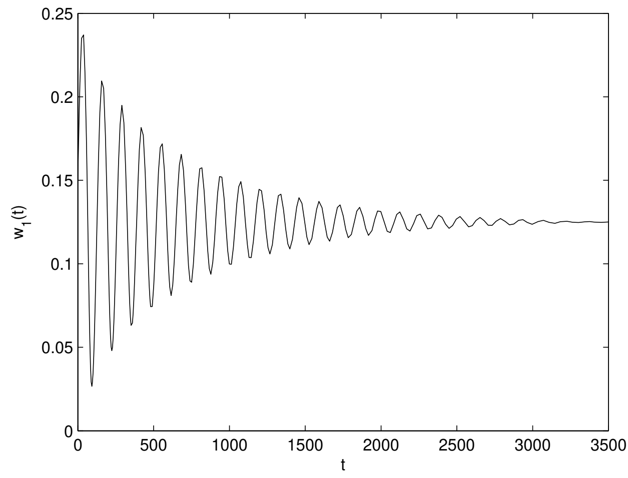

Figure 1. Software experiment outcomes of system (81) concerning the time delay $\vartheta = 4.5 < \vartheta_0 = 5.3$. The positive equilibrium point $W(0.1250, 0.5830)$ preserves locally asymptotically stable situation. x-axis stands for t and y-axis stands for $w_1(t)$.

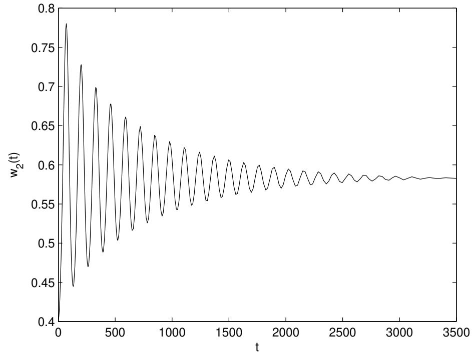

Figure 2. Software experiment outcomes of system (81) concerning the time delay $\vartheta = 4.5 < \vartheta_0 = 5.3$. The positive equilibrium point $W(0.1250, 0.5830)$ preserves locally asymptotically stable situation. x-axis stands for t and y-axis stands for $w_2(t)$.

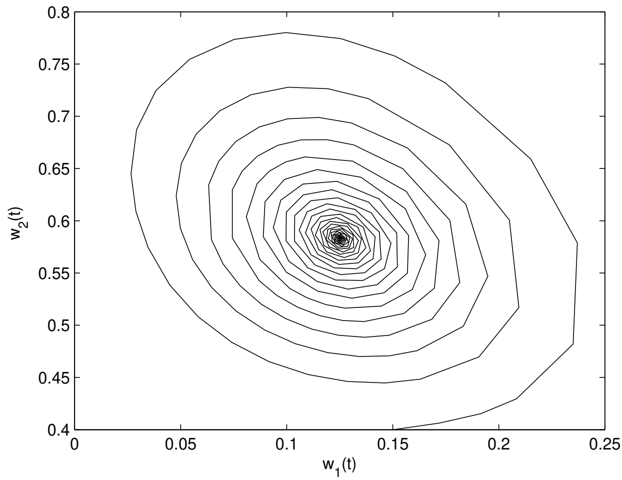

Figure 3. Software experiment outcomes of system (81) concerning the time delay $\vartheta = 4.5 < \vartheta_0 = 5.3$. The positive equilibrium point $W(0.1250, 0.5830)$ preserves locally asymptotically stable situation. x-axis stands for $w_1(t)$ and y-axis stands for $w_2(t)$.

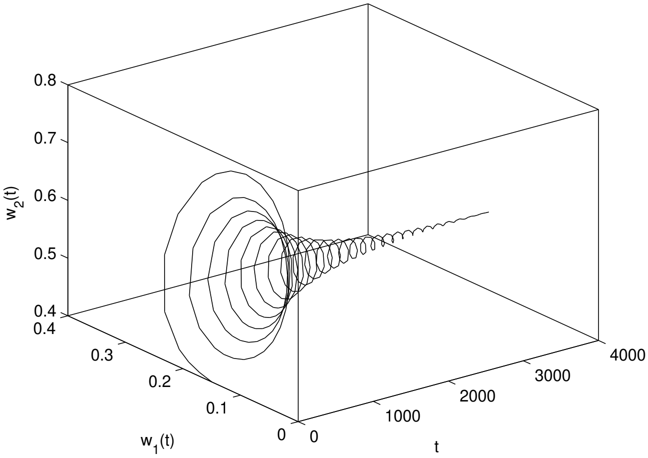

Figure 4. Software experiment outcomes of system (81) concerning the time delay $\vartheta = 4.5 < \vartheta_0 = 5.3$. The positive equilibrium point $W(0.1250, 0.5830)$ preserves locally asymptotically stable situation. x-axis stands for t, y-axis stands for $w_1(t)$ and z-axis stands for $w_2(t)$.

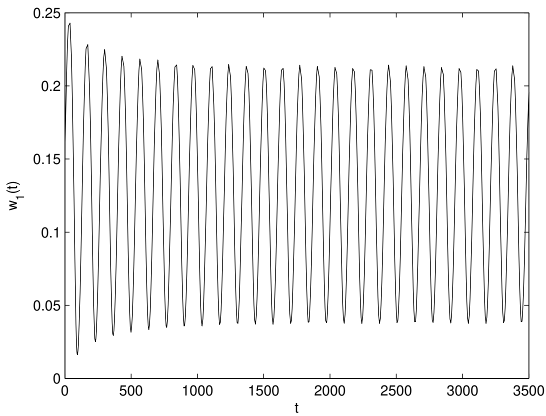

Figure 5. Software experiment outcomes of system (81) concerning the time delay $\vartheta = 6.5 > \vartheta_0 = 5.3$. A cluster of limit cycles (Hopf bifurcations) happen around the positive equilibrium point $W(0.1250, 0.5830)$. x-axis stands for t and y-axis stands for $w_1(t)$.

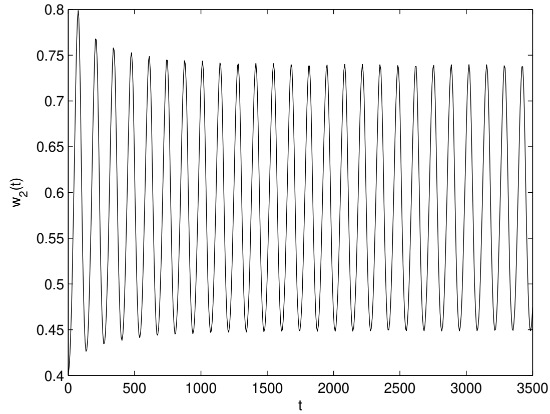

Figure 6. Software experiment outcomes of system (81) concerning the time delay $\vartheta = 6.5 > \vartheta_0 = 5.3$. A cluster of limit cycles (Hopf bifurcations) happen around the positive equilibrium point $W(0.1250, 0.5830)$. x-axis stands for t and y-axis stands for $w_2(t)$.

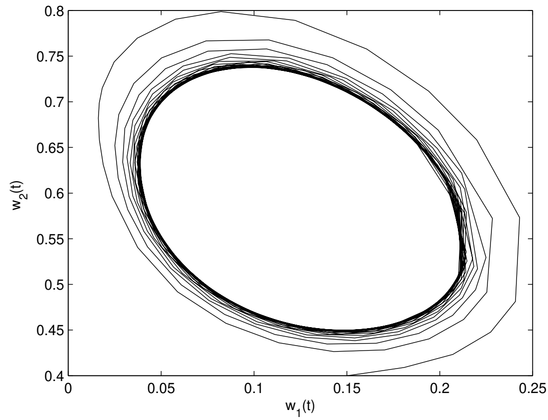

Figure 7. Software experiment outcomes of system (81) concerning the time delay $\vartheta = 6.5 > \vartheta_0 = 5.3$. A cluster of limit cycles (Hopf bifurcations) happen around the positive equilibrium point $W(0.1250, 0.5830)$. x-axis stands for $w_1(t)$ and y-axis stands for $w_2(t)$.

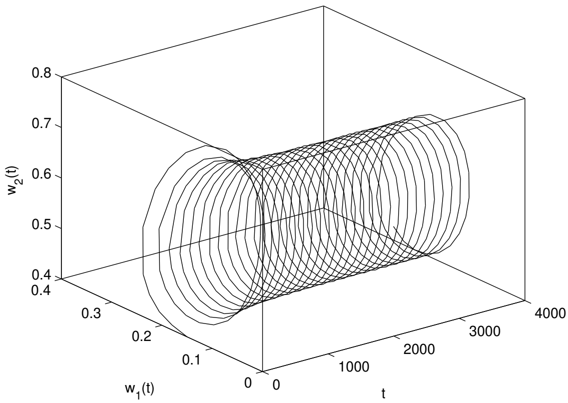

Figure 8. Software experiment outcomes of system (81) concerning the time delay $\vartheta = 6.5 > \vartheta_0 = 5.3$. A cluster of limit cycles (Hopf bifurcations) happen around the positive equilibrium point $W(0.1250, 0.5830)$. x-axis stands for t, y-axis stands for $w_1(t)$ and z-axis stands for $w_2(t)$.

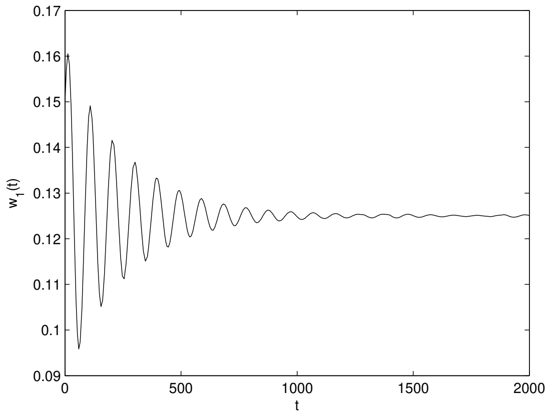

Figure 9. Software experiment outcomes of system (82) concerning the time delay $\vartheta = 2.1 < \vartheta_* = 2.5$. The positive equilibrium point $W(0.1250, 0.5830)$ preserves locally asymptotically stable situation. x-axis stands for t and y-axis stands for $w_1(t)$.

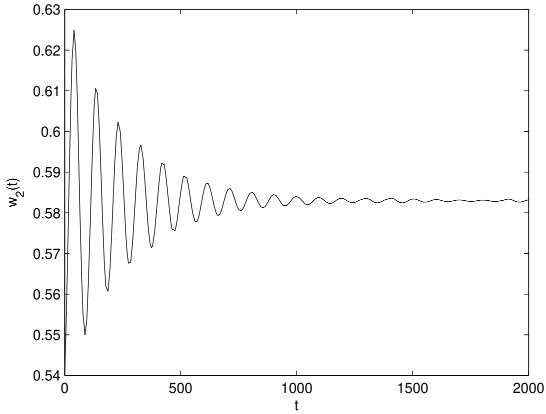

Figure 10. Software experiment outcomes of system (82) concerning the time delay $\vartheta = 2.1 < \vartheta_* = 2.5$. The positive equilibrium point $W(0.1250, 0.5830)$ preserves locally asymptotically stable situation.x-axis stands for t and y-axis stands for $w_2(t)$.

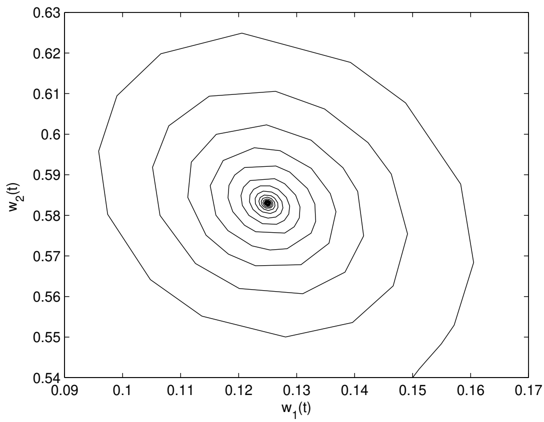

Figure 11. Software experiment outcomes of system (82) concerning the time delay $\vartheta = 2.1 < \vartheta_* = 2.5$. The positive equilibrium point $W(0.1250, 0.5830)$ preserves locally asymptotically stable situation. x-axis stands for $w_1(t)$ and y-axis stands for $w_2(t)$.

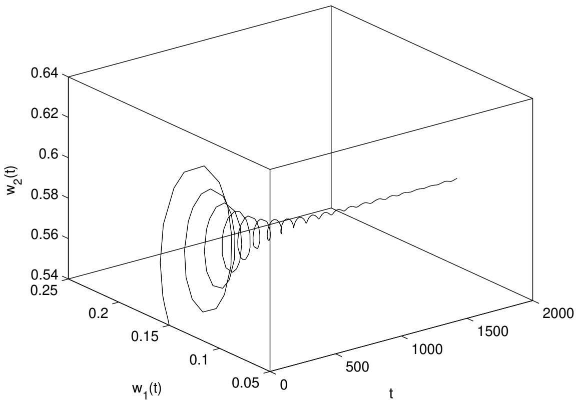

Figure 12. Software experiment outcomes of system (82) concerning the time delay $\vartheta = 2.1 < \vartheta_* = 2.5$. The positive equilibrium point $W(0.1250, 0.5830)$ preserves locally asymptotically stable situation. x-axis stands for t, y-axis stands for $w_1(t)$ and z-axis stands for $w_2(t)$.

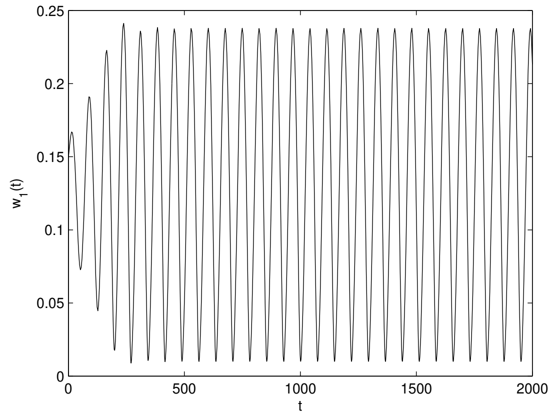

Figure 13. Software experiment outcomes of system (82) concerning the time delay $\vartheta = 3.5 > \vartheta_* = 2.5$. A cluster of limit cycles (Hopf bifurcations) happen around the positive equilibrium point $W(0.1250, 0.5830)$. x-axis stands for t and y-axis stands for $w_1(t)$.

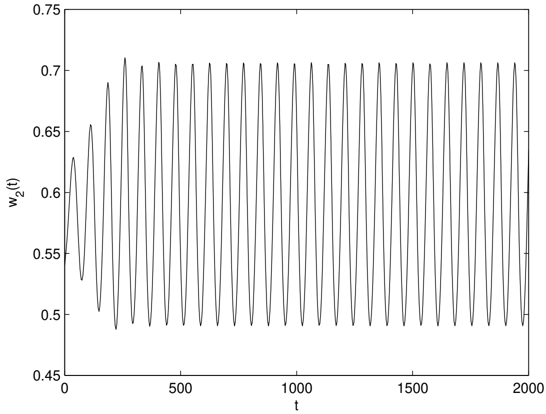

Figure 14. Software experiment outcomes of system (82) concerning the time delay $\vartheta = 3.5 > \vartheta_* = 2.5$. A cluster of limit cycles (Hopf bifurcations) happen around the positive equilibrium point $W(0.1250, 0.5830)$. x-axis stands for t and y-axis stands for $w_2(t)$.

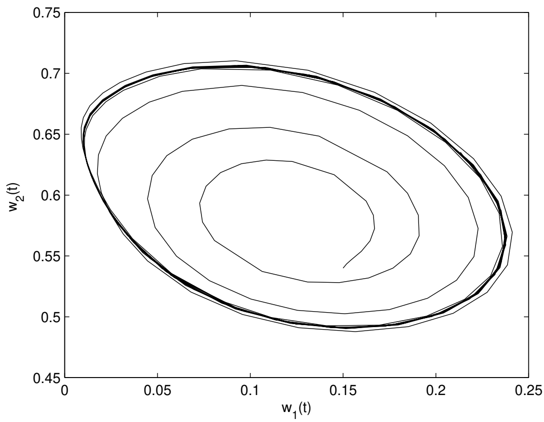

Figure 15. Software experiment outcomes of system (82) concerning the time delay $\vartheta = 3.5 > \vartheta_* = 2.5$. A cluster of limit cycles (Hopf bifurcations) happen around the positive equilibrium point $W(0.1250, 0.5830)$. x-axis stands for $w_1(t)$ and y-axis stands for $w_2(t)$.

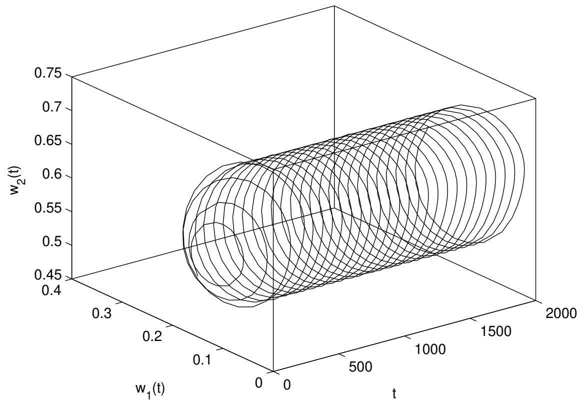

Figure 16. Software experiment outcomes of system (82) concerning the time delay $\vartheta = 3.5 > \vartheta_* = 2.5$. A cluster of limit cycles (Hopf bifurcations) happen around the positive equilibrium point $W(0.1250, 0.5830)$. x-axis stands for t, y-axis stands for $w_1(t)$ and z-axis stands for $w_2(t)$.

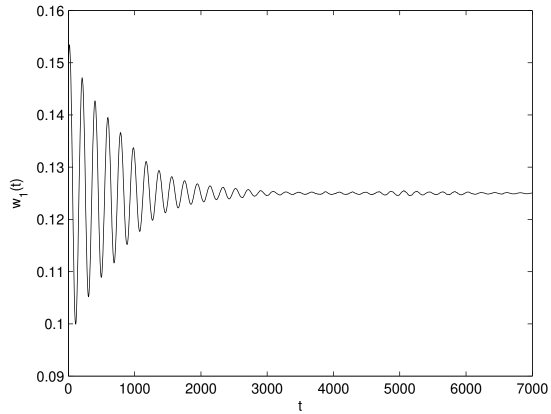

Figure 17. Software experiment outcomes of system (83) concerning the time delay $\vartheta = 1.98 < \vartheta_{*0} = 2.1$. The positive equilibrium point $W(0.1250, 0.5830)$ preserves locally asymptotically stable situation. x-axis stands for t and y-axis stands for $w_1(t)$.

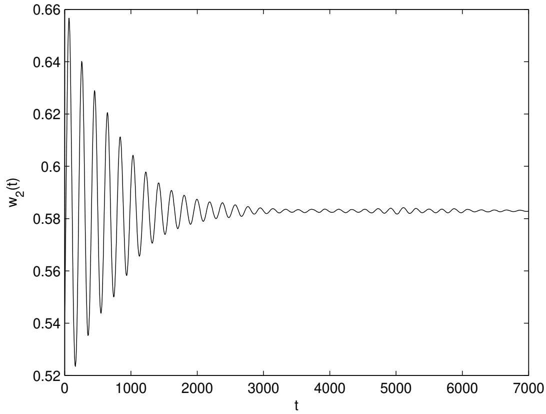

Figure 18. Software experiment outcomes of system (83) concerning the time delay $\vartheta = 1.98 < \vartheta_{*0} = 2.1$. The positive equilibrium point $W(0.1250, 0.5830)$ preserves locally asymptotically stable situation. x-axis stands for t and y-axis stands for $w_2(t)$.

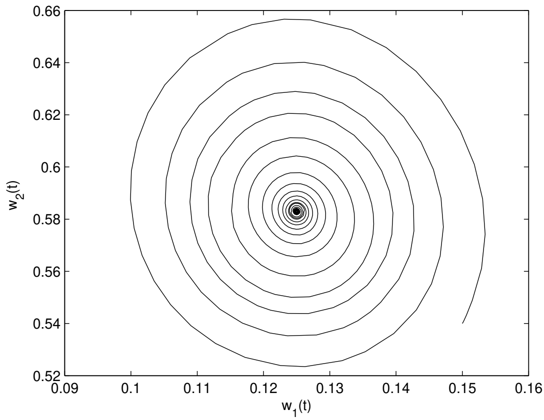

Figure 19. Software experiment outcomes of system (83) concerning the time delay $\vartheta = 1.98 < \vartheta_{*0} = 2.1$. The positive equilibrium point $W(0.1250, 0.5830)$ preserves locally asymptotically stable situation. x-axis stands for $w_1(t)$ and y-axis stands for $w_2(t)$.

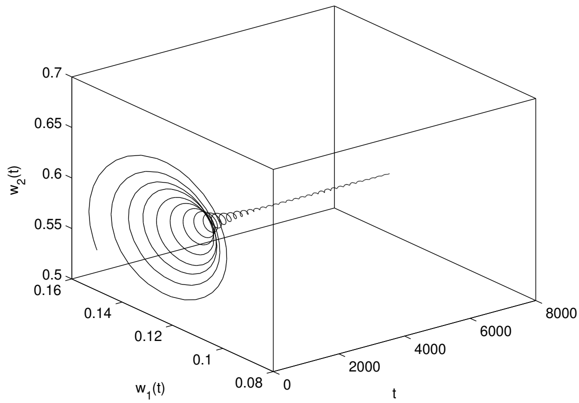

Figure 20. Software experiment outcomes of system (83) concerning the time delay $\vartheta = 1.98 < \vartheta_{*0} = 2.1$. The positive equilibrium point $W(0.1250, 0.5830)$ preserves locally asymptotically stable situation. x-axis stands for t, y-axis stands for $w_1(t)$ and z-axis stands for $w_2(t)$.

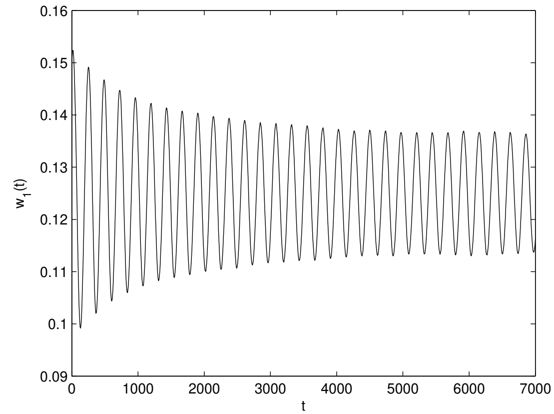

Figure 21. Software experiment outcomes of system (83) concerning the time delay $\vartheta = 2.25 > \vartheta_{*0} = 2.1$. A cluster of limit cycles (Hopf bifurcations) happen around the positive equilibrium point $W(0.1250, 0.5830)$. x-axis stands for t and y-axis stands for $w_1(t)$.

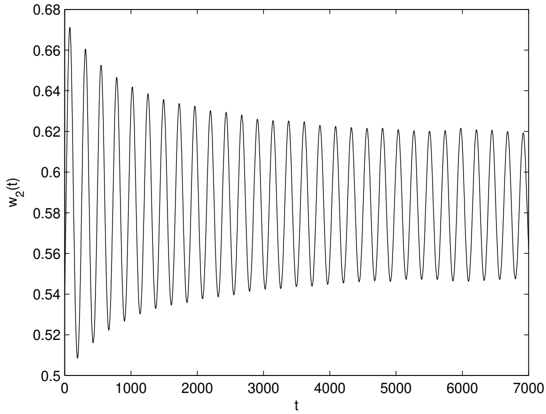

Figure 22. Software experiment outcomes of system (83) concerning the time delay $\vartheta = 2.25 > \vartheta_{*0} = 2.1$. A cluster of limit cycles (Hopf bifurcations) happen around the positive equilibrium point $W(0.1250, 0.5830)$. x-axis stands for t and y-axis stands for $w_1(t)$.

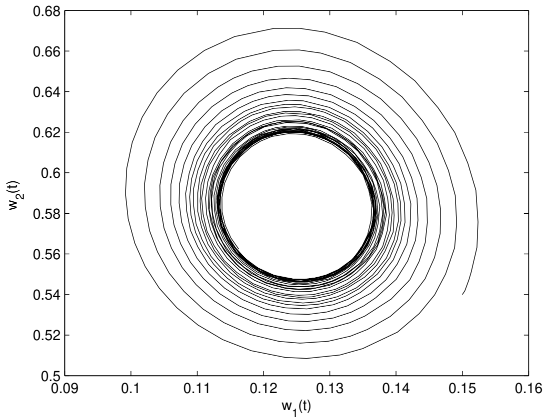

Figure 23. Software experiment outcomes of system (83) concerning the time delay $\vartheta = 2.25 > \vartheta_{*0} = 2.1$. A cluster of limit cycles (Hopf bifurcations) happen around the positive equilibrium point $W(0.1250, 0.5830)$. x-axis stands for $w_1(t)$ and y-axis stands for $w_2(t)$.

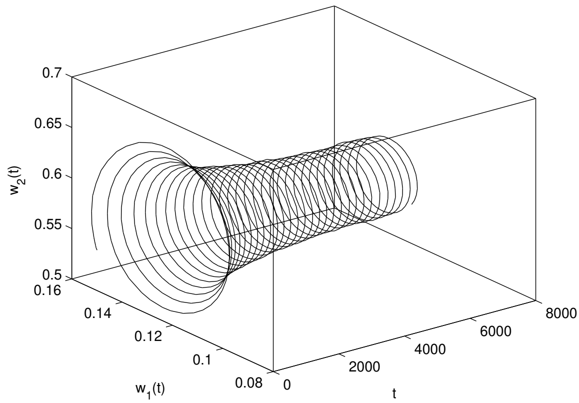

Figure 24. Software experiment outcomes of system (83) concerning the time delay $\vartheta = 2.25 > \vartheta_{*0} = 2.1$. A cluster of limit cycles (Hopf bifurcations) happen around the positive equilibrium point $W(0.1250, 0.5830)$. x-axis stands for t, y-axis stands for $w_1(t)$ and z-axis stands for $w_2(t)$.

Remark 6.1. *From the simulation figures of Example (81)-(83), we obtain the bifurcation delay value of Example (81)-(83) are* 5.3, 2.5, 2.1, *respectively. It means that we can narrowed the stability domain of system (81) postpone the time of emergence of Hopf bifurcation of system (81) via our designed extended hybrid controller I and extended hybrid controller II.*

7 Conclusions

Setting up proper mathematical models to describe various chemical reaction laws play a vital role in chemistry. By virtue of exploring the established mathematical models, we can effectively reveal the development laws of different chemical compositions and then serve humanity better. In this work, we have explored the existence and uniqueness, non-negativeness, boundedness of the solution of a delayed chemostat model by using fixed point theorem, inequality strategies and construction of a suitable function. By taking the delay as parameter and analyzing the characteristic equation of the model, we establish a new delay-independent bifurcation and stability condition for this model. In order to adjust the stability domain and the time of emergence of bifurcation of the model, we take two effective extended hybrid controllers to achieve our goal. The study manifests that delay is a vital factor which affect the stability and bifurcation of the model. The acquires outcomes own very important theoretical value in controlling and balancing the concentrations of various chemical substances. Furthermore, the exploration ideas can be useful in dealing with the control issue of bifurcation of numerous differential models.

***Acknowledgment*:** This work is supported by National Natural Science Foundation of China (No.12261015) and Innovative Exploration Project of Guizhou University of Finance and Economics(2022XSXMA08).

References

[1] Z. Eskandari, R. K. Ghaziani, Z. Avazzadeh, B. Li, Codimension-2 bifurcation on the curve of the Neimark-Sacker bifurcation for a discrete-time chemical model, *J. Math. Chem.* (2023) doi: https://doi.org/10.1007/s10910-023-01449-9

[2] C. H. Zhang, Y. He, Multiple stability switches and Hopf bifurcations induced by the delay in a Lengyel-Epstein chemical reaction system, *Appl. Math. Comput.* **378** (2020) #125201.

[3] C. J. Xu, Y. S. Wu, Bifurcation and control of chaos in a chemical system, *Appl. Math. Model.* **39** (2015) 2295–2310.

[4] I. Lengyel, G. Ribai, I. R. Epstein, Experimental and modeling study of oscillations in the chlorine dioxide-iodine-malonic acid reaction, *J. Am. Chem. Soc.* **112** (1990) 9104–9110.

[5] Q. Din, T. Donchev, D. Kolev, Stability, bifurcation analysis and chaos control in chlorine dioxide-iodine-malonic acid reaction, *MATCH Commun. Math. Comput. Chem.* **79** (2018) 577–606.

[6] C. J. Xu, D. Mu, Z. X. Liu, Y. C. Pang, M. X. Liao, P. L. Li, Bifurcation dynamics and control mechanism of a fractional-order delayed Brusselator chemical reaction model, *MATCH Commun. Math. Comput. Chem.* **89** (2023) 73–106.

[7] D. Mu, C. J. Xu, Z. X. Liu, Y. C. Pang, Further insight into bifurcation and hybrid control tactics of a chlorine dioxide-iodine-malonic acid chemical reaction model incorporating delays, *MATCH Commun. Math. Comput. Chem.* **89** (2023) 529–566.

[8] C. J. Xu, C. Aouiti, Z. X. Liu, P. L. Li, L. Y. Yao, Bifurcation caused by delay in a fractional-order coupled Oregonator model in chemistry, *MATCH Commun. Math. Comput. Chem.* **88** (2022) 371–396.

[9] C. J. Xu, W. Zhang, C. Aouiti, Z. X. Liu, P. L. Li, Bifurcation dynamics in a fractional-order Oregonator model including time delay, *MATCH Commun. Math. Comput. Chem.* **87** (2022) 397–414.

[10] N. A. Mohd Aris, S. S. Jamaian, Dynamical analysis of fractional-order chemical model, *AIMS Biophys.* **8** (2021) 182–197.

[11] S. L. Yuan, P. Li, Y. L. Song, Delay induced oscillations in a turbidostat with feedback control, *J. Math. Chem.* **49** (2011) 1646–1666.

[12] V. Voorsluijs, Y. D. Decker, Emergence of chaos in a spatially confined reactive system, *Phys. D* **335** (2016) 1–9.

[13] M. I. Nelson, H. S. Sidhu, Analysis of a chemostat modelwith variable yield coefficient, *J. Math. Chem.* **38** (2005) 605–615.

[14] N. A. Mohd Aris, S. S. Jamaian, Stability analsyis of fractional-order chemostat model with time delay, in: A. B. Mustapha, S. Shamsuddin, S. Z. H. Rizvi, S. B. Asman, S. S. Jamaian (Eds.), *Proceedings of the 7th International Conference on the Applications of Science and Mathematics 2021*, Springer, Singapore, 2022, pp. 213–228.

[15] C. J. Xu, W. Zhang, C. Aouiti, Z. X. Liu, L. Y. Yao, Bifurcation insight for a fractional-order stage-structured predator-prey system incorporating mixed time delays, *Math. Meth. Appl. Sci.* **46** (2023) 9103–9118.

[16] C. J. Xu, D. Mu, Z. X. Liu, Y. C. Pang, M. X. Liao, C. Aouiti, New insight into bifurcation of fractional-order 4D neural networks incorporating two different time delays, *Comm. Nonlin. Sci. Num. Sim.* **118** (2023) #107043.

[17] C. J. Xu, Z. X. Liu, P. L. Li, J. L. Yan, L. Y. Yao, Bifurcation mechanism for fractional-order three-triangle multi-delayed neural networks, *Neural Proc. Lett.* (2023) https://doi.org/10.1007/s11063-022-11130-y

[18] C. J. Xu, D. Mu, Z. X. Liu, Y. C. Pang, M. X. Liao, P. L. Li, L. Y. Yao, Q. W. Qin, Comparative exploration on bifurcation behavior for integer-order and fractional-order delayed BAM neural networks, *Nonlin. Anal. Model. Control* **27** (2022) 1030–1053.

[19] C. J. Xu, Z. X. Liu, Y. C. Pang, S. Saifullah, J. Khan, Torus and fixed point attractors of a new multistable hyperchaotic 4D system, *J. Comput. Sci.* **67** (2023) #101974.

[20] C. J. Xu, Z. X. Liu, M. X. Liao, L. Y. Yao, Theoretical analysis and computer simulations of a fractional order bank data model incorporating two unequal time delays, *Expert Sys. Appl.* **199** (2022) #116859.

[21] H. L. Li, L. Zhang, C. Hu, Y. L. Jiang, Z. D. Teng, Dynamical analysis of a fractional-order prey-predator model incorporating a prey refuge, *J. Appl. Math. Comput.* **54** (2017) 435–449.

[22] M. Das, A. Maiti, G. P. Samanta, Stability analysis of a prey-predator fractional order model incorporating prey refuge, *Ecol. Genet. Genom.* **7-8** (2018) 33–46.

[23] S. Y. Lin, New results for generalised Gronwall inequality and their application, *Abst. Appl. Anal.* **2014** (2014) # 168594.

[24] Z. Z. Zhang, H. Z. Yang, Hybrid control of Hopf bifurcation in a two prey one predator system with time delay, *Proceeding of the 33rd Chinese Control Conference, July 28-30*, Nanjing, 2014, pp. 6895–6900.

[25] L. P. Zhang, H. N. Wang, M. Xu, Hybrid control of bifurcation in a predator-prey system with three delays, *Acta Phys. Sinica* **60** (2011) #010506.

[26] Z. Liu, K. W. Chuang, Hybrid control of bifurcation in continuous nonlinear dynamical systems, *Int. J. Bifur. Chaos* **15** (2005) 1895–3903.

[27] W. C. Xie, Y. M. Sun, A new result on PD controller design for second order nonlinear uncertain systems, *J. Franklin Inst.* **359** (2022) 7307–7318.

[28] R. Y. Zhang, Bifurcation analysis for T system with delayed feedback and its application to control of chaos, *Nonlin. Dyn.* **72** (2013) 629–641.

[29] M. Xiao, D. W. C. Ho, J. D. Cao, Time-delayed feedback control of dynamical small-world networks at Hopf bifurcation, *Nonlin. Dyn.* **58** (2009) 319–344.